Chinese Chemical Letters 34 (2023) 107904

Contents lists available at ScienceDirect

Chinese Chemical Letters

journal homepage: www.elsevier.com/locate/cclet

Recent advances in photoelectrochemical sensors for detection of ions in water

Linyang Li[a], Junlian Chen[a], Chuanbao Xiao[a], Yihao Luo[b], Nianbing Zhong[a,b,*], Quanhua Xie[a], Haixing Chang[c,**], Dengjie Zhong[c], Yunlan Xu[c], Mingfu Zhao[a], Qiang Liao[d,**]

[a] Intelligent Fiber Sensing Technology of Chongqing Municipal Engineering Research Center of Institutions of Higher Education, Chongqing Key Laboratory of Modern Photoelectric Detection Technology and Instrument, Chongqing Key Laboratory of Fiber Optic Sensor and Photodetector, Chongqing University of Technology, Chongqing 400054, China
[b] Biodesign Swette Center for Environmental Biotechnology, Arizona State University, Tempe, AZ 85271-5701, United States
[c] College of Chemistry and Chemical Engineering, Chongqing University of Technology, Chongqing 400054, China
[d] Key Laboratory of Low-grade Energy Utilization Technologies and Systems (Chongqing University), Ministry of Education, Chongqing 400030, China

ARTICLE INFO

Article history:
Received 14 June 2022
Revised 25 September 2022
Accepted 13 October 2022
Available online 17 October 2022

Keywords:
Photoelectrochemical sensor
Ion detection
Working principle
Electronic transfer
Sensitivity and selectivity
Limit of detection

ABSTRACT

Over the last 50 years, the explosive adoption of modern agricultural practices has led to an enormous increase in the emission of non-biodegradable and highly biotoxic ions into the hydrosphere. Excess intake of such ions, even essential trace elements such as Cu^{2+} and F^{-}, can have serious consequences on human health. Therefore, to ensure safe drinking water and regulate wastewater discharge, photoelectrochemical (PEC) online sensors were developed, with advantages such as low energy consumption, inherent miniaturization, simple instrumentation, and fast response. However, there is no publicly available systematic review of the recent advances in PEC ion sensors available in the literature since January 2017. Thus, this review covers the various strategies that have been used to enhance the sensitivity, selectivity, and limit of detection for PEC ion sensors. The photoelectrochemically active materials, conductive substrates, electronic transfer, and performance of various PEC sensors are discussed in detail and divided into sections based on the measurement principle and detected ion species. We conclude this review by highlighting the challenges and potential future avenues of research associated with the development of novel high-performance PEC sensors.

1. Introduction

Ion-sensing technology has expanded in the last 50 years with increasing demands for water quality detection as numerous ions and their compounds are being discharged into water sources due to anthropogenic activities [1–3]. However, ions are commonly found in the human body and nature, but it is their imbalance or contamination in nature/human body that can be detrimental [4–7]. For example, trace elements (Cu^{2+} and F^{-}) are generally beneficial for the human body at low concentrations and will cause poisoning and related physiological diseases at higher dodes [8–10]. On the contrary, heavy metal and redox (NO_2^{-}) ions are harmful to humans in even small quantities [11,12]. Importantly, their contamination in environment is irreversible, can get accumulated, and has an indelible impact on the biosphere [13–15]. Therefore, to ensure safe drinking water and guide wastewater discharge, it is necessary to develop advanced sensors for the detection of trace ion concentrations in water [16–20].

Numerous online sensors such as fiber-optic, electrochemical, and photoelectrochemical (PEC) sensors have been developed because of their simple design, low cost, fast response, easy operation, portability, and the ability to enable selective and *in-situ* real-time detection [21–23]. Of the sensors, PEC sensing is a promising analytical technology because of its high sensitivity, rapid response, low energy consumption, inherent miniaturization, and simple instrumentation [24–27].

* Corresponding author at: Intelligent Fiber Sensing Technology of Chongqing Municipal Engineering Research Center of Institutions of Higher Education, Chongqing Key Laboratory of Modern Photoelectric Detection Technology and Instrument, Chongqing Key Laboratory of Fiber Optic Sensor and Photodetector, Chongqing University of Technology, Chongqing 400054, China.
** Corresponding authors.
E-mail addresses: zhongnianbing@163.com (N. Zhong), changhx@cqut.edu.cn (H. Chang), lqzx@cqu.edu.cn (Q. Liao).

https://doi.org/10.1016/j.cclet.2022.107904
1001-8417/

Until now, numerous novel PEC sensors have been proposed for the detection of ions in wastewater [28–36]. Most previous works have mainly focused on improving the performance of photoelectrochemical materials to extend visible-light absorption, enhance photoelectric conversion, influence charge recombination kinetics, and thus increase the magnitude of changes in photocurrent [36–39]. With the emergence of a variety of ions in wastewater, efforts should be made to carefully study the mechanism of ion selectivity measurement as the ion-selective adsorption of photoelectrochemically active materials is often unsatisfactory. In addition, the principles and methods to extend the detection range and improve the low limit of detection (LOD) of the PEC ion sensors should be also illustrated. However, these important properties—the preparation, measurement principle, and performance—of PEC ion sensors for selective monitoring trace metal and non-metal ions in water have not yet been systematically reviewed. Furthermore, the last comprehensive review of PEC metal-ion sensors (eight ions: Cu^{2+}, Cr^{6+}, Hg^{2+}, Pb^{2+}, Ag^{+}, K^{+}, Ca^{2+}, and Cd^{2+}) was published in 2016 [40] and a review of PEC biosensors for detection of four heavy metal ions (Hg^{2+}, Pb^{2+}, Ag^{+}, and K^{+} ions) was reported in 2018 (The reported review is based on selecting the papers published in 2009–2016) [41]; a review of PEC sensors for non-metal-ion detection has not yet been reported yet.

The goal of this review is to address the aforementioned issues and provide a comprehensive discussion on all PEC ion sensors developed between January 2017 and June 2022. Section 2 covers the principles employed for measurement of ions in water. Sections 3 and 4 describe the composition (of the ion-selective sensitive photoelectrode) and performance (sensitivity, selectivity, detection range, and LOD) of 9 metal-ion (Cu^{2+}, Cr^{6+}, Hg^{2+}, Pb^{2+}, Ag^{+}, K^{+}, Co^{2+}, As^{5+}, and Tl^{+}) and 3 non-metal-ion (NO_2^{-}, F^{-}, and S^{2-}) PEC sensors. Finally, achievements and outlook of PEC ion sensors are discussed.

2. Working principle of PEC sensors

In general, a PEC sensing system is composed of a three-electrode subsystem, a light source (such as Xe lamp, halogen lamp, and light emitting diode), and an electrochemical workstation. The electrode subsystem includes a reference electrode (RE), counter electrode (CE), and working electrode (WE). The RE is usually an Ag/AgCl electrode or a saturated calomel electrode, the CE is generally a platinum electrode, and the WE is composed of photoelectrochemical materials and conductive substrates such as indium tin oxide (ITO) glass. The light source was used to irradiate the working electrode and produce photocurrent readout signal. The photocurrents are recorded by an electrochemical workstation (Fig. 1).

In PEC sensors, a series of conversion and transfer processes occur between light, photoelectrochemical materials, conductive substrates, and the target analyte. First, the electrons of photoelectrochemical materials get excited by light and migrate from valence band (VB) to conduction band (CB) to form electron-hole pairs. Once this process occurs, there are two choices for the transfer of CB electrons: recombine or transfer charges outside [42]. The transport path of CB electrons will affect the polarity of photocurrent, mainly cathode photocurrent and anode photocurrent (Fig. 1) [43]. Second, when the CB electrons are transferred to the electrolyte and react with the electron acceptor in the electrolyte solution, the electrons on the electrode surface are transferred to the holes generated by the VB and yield a cathodic photocurrent. Third, when the CB electrons are further transferred to the electrode surface and the electrons in the electrolyte solution are transferred to the holes in the VB, an anodic photocurrent is generated [44]. The photocurrent generated *via* light excitation will be affected by the ion concentration in analyte, resulting in changes in photocurrent

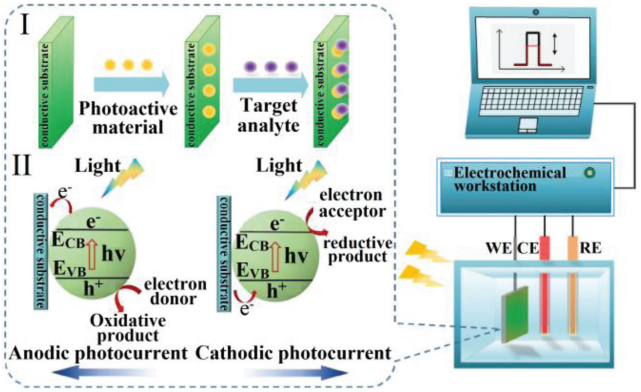

Fig. 1. Schematic of PEC sensor: (I) Working principle of PEC detection. (II) The photocurrent generation mechanism. Copied with permission [43]. Copyright 2020, the Royal Society of Chemistry.

(such as photocurrent increases, photocurrent decreases, or switch in photocurrent polarity) that can be utilized for determining an ion's concentration [45]. Herein, these three measurement principles are discussed in detail.

2.1. Measurement based on decrease in photocurrent

Numerous PEC ion sensors are available that detect the target analyte based on the decrease in photocurrent generated by light excitation; these are named "signal-off" PEC ion sensors. The five most common conditions that cause a decrease in the generated photocurrent are as follows: (a) The target analyte reacts with the photoelectrochemically active material, resulting in the production of new species on the electrode surface (such as Cu_xS [46], Cu_7S_4 [47], Co-CS chelate [36]), which inhibits electron transport and decreases photocurrent. (b) The target analyte reacts with the photoelectrochemically active material, thereby disrupting or inhibiting certain reactions (such as the hybridization between aptamer and DNA) [48] and resulting in a decrease in photocurrent [48]. (c) Energy transfer (such as between CdS quantum dots and Au nanoparticles) occurs in the presence of target analyte, resulting in a decrease in photocurrent [49]. (d) The interaction between the target analyte and the hole scavenger in the electrolyte destroys the electron transfer between the hole scavenger and the hole, resulting in a decrease in photocurrent [50]. (e) The target analyte triggers the dissolution or surface state passivation of the photoelectrochemically active materials, thereby resulting in a decrease of photocurrent [51].

2.2. Measurement based on increase in photocurrent

Some PEC sensors produce an increase in photocurrent with increasing ion concentration; such devices and are known as "signal-on" PEC ion sensors. The increase in photocurrent is controlled by the photosensitive material, the probe ion species, and their interactions; the four cases are described as follows: (a) The target analyte reacts with photoelectrochemically active materials (such as ZnO [34], ZnS@Ag_2S [52]) and the reaction products are coated on the electrode surface to form the new heterojunction (HgS/ZnS@Ag_2S) [52] or photosensitizer (CdSe [33], AgBr [34]); the heterojunction can promote the separation of electron-hole pairs under light illumination and the photosensitizer can enhance light absorption to prompt the generation of electron-hole pairs, thereby resulting in an increase in photocurrent. (b) In the presence of the target analyte, the analyte can destroy or inhibit the reaction (such as energy transfer [53], generation of insoluble products [54]) and restore the decreased photocurrent, that is, the photocurrent in-

creases. (c) In PEC sensors, the charge carrier reacts directly with the target analyte to decrease the recombination of electron-hole pairs, thereby speeding up the transfer rate of photogenerated carriers and leading to an increase in photocurrent [55,56]. (d) The target analyte can change the structure or state of photoelectrochemically active materials (such as the formation of folding configuration [57], the restoration of oxidation state [58], the formation of heterojunction [59]), so as to increase the photocurrent.

2.3. Measurement based on polarity-switchable photocurrent

In recent years, PEC ion sensors with target analyte induced polarity-switchable effect in photocurrent have been developed [60–62]. The photocurrent of such sensors changes in two ways: (a) When the concentration of the target analyte increases, the photocurrent continuously decreases to zero and finally increases in reverse; (b) when the target analyte exists, it directly leads to the switching of photocurrent polarity. The reverse change in photocurrent is generally caused by competitive reactions (such as the competition between the photoreactions reactions at the surface of the photoelectrochemically active materials and the charge carrier transfer process of the electrode [61,62] or the competitive adsorption between the target analyte and photoelectrochemically active materials [60]).

3. PEC sensors for metal ions

Although the change in photocurrent generated in PEC ion sensors shows three patterns, as discussed in Section 2, such changes are simultaneously affected by the electrode active material, the target detection ion species, and their interactions. PEC sensors with same photoelectrochemically active material (such as n-type and p-type semiconductors and DNA probe) for the detection different ions show different changes in photocurrent; similarly, when the detection ion is given, PEC sensors with different active materials also show different changes in photocurrent. Therefore, to clearly describe the research progress in PEC ion sensors, instead of classifying them based on the way the photocurrent changes, they will be classified according to ion species here. Furthermore, the composition, active materials, the way in which the generated photocurrent changes with increasing ion concentration, and performance of the PEC sensors are discussed in detail.

3.1. Detection of Cu^{2+}

Cu^{2+} is the third most essential trace element in the human body and an essential dietary mineral for organisms; it thus plays a vital role in heme formation, iron absorption, and so on [63]. Although many reactions of copper ions are indispensable, abnormal ingestion of Cu^{2+} leads to protein denaturation and inactivation, leading to Wilson, Alzheimer's disease, and other diseases [64]. The recommended intake of Cu^{2+} for adults is approximately 0.8–0.9 mg/day, while the drinking-water quality guidelines of the World Health Organization (WHO 2008) recommend that the copper content must be limited to 20 μmol/L. Therefore, accurate monitoring of Cu^{2+} concentration is very important.

3.1.1. CdS-based PEC sensors for detection of Cu^{2+}

CdS is a typical n-type semiconductor and has been widely used in PEC sensors on account of its suitable band gap and strong absorption of visible light. In PEC Cu^{2+} sensors, when the CdS-based Cu^{2+} sensitive materials coated ITO and FTO electrodes come in contact with the Cu^{2+}-containing solutions, Cu_xS ($x = 1,2$) is formed on their surface due to the excellent selective interaction between CdS and Cu^{2+} ions, which not only blocks the light illumination paths but also promotes the recombination of photogenerated carriers, thereby causing photocurrent quenching. Therefore, sensors with CdS-based ITO mediated electrodes can be used to linearly detect Cu^{2+} ion concentration.

PEC Cu^{2+} sensing technology based on CdS was first proposed by Wang *et al.* in 2010 [46]; subsequently, CdS (n-type semiconductor) has been widely used in PEC sensors on account of its suitable band gap and strong absorption of visible light [29,38,39,65–67]. However, PEC sensors with pure CdS-coated electrodes show low sensitivity to Cu^{2+} due to the rapid recombination of electron-hole pairs in the pure CdS sensitive material before migrating to the surface. Therefore, to improve sensitivity of PEC sensors to Cu^{2+} ions, the pure CdS sensitive material was replaced with a CdS complex to promote the separation of photogenerated carriers. For example, Wang *et al.* proposed WO_3/CdS heterostructure sensitive films (Fig. 2a) and investigated the sensitivity and anti-interference ability of a PEC sensor with fluorine-doped tin oxide (FTO)/WO_3/CdS electrode for diverse metal ions [39]. Under illumination, photogenerated electrons migrate from CB of CdS to WO_3 because CB and VB of CdS are more negative than those of WO_3. At the same time, holes migrate from VB of WO_3 to CdS. When Cu^{2+} exists, some electron-hole pairs are transferred to Cu_xS ($x = 1$, 2), promoting the surface charge recombination of WO_3/CdS electrode, and the photocurrent density decreases. The LOD and linear range of this sensor are 0.06 μmol/L and 0.5 μmol/L∼1 mmol/L, respectively.

In CdS-based Cu^{2+} PEC sensors, combinations of CdS and other materials, such as BiOI [29], CuS [38], ZnO [66]), Ti_3C_2 [67], TiO_2 [65], graphene [68], ZnO-graphene [69], and cellulose acetate (Fig. 2b) [70], have been continuously developed. Moreover, considerable research efforts have been made toward assembling Au on the surface of CdS sensing material to prepare PEC sensors, because the assembly of noble metals on the surface of semiconductor materials can effectively inhibit the recombination of electron-hole pairs and improve sensitivity [71]. Furthermore, the rapid recombination of photogenerated carriers of CdS-based materials can also be inhibited by improving the surface area of the support materials. Graphene has become a good choice because of the high surface area of single-layer graphene. Herein, the introduction of graphene into CdS can enhance the sensitivity of CdS-based PEC sensors for detection of Cu^{2+} ions [72].

3.1.2. g-C_3N_4-based PEC sensors for detection of Cu^{2+}

Graphite carbon nitride (g-C_3N_4) is a type of polymer semiconductor material, PEC sensors with g-C_3N_4-coated electrodes have been widely applied for the detection of Cu^{2+} concentration due to the visible-light response, unique electronic band structure, nontoxic, and low cost of g-C_3N_4. Unfortunately, due to the high recombination rate of photogenerated electron-hole pairs and low specific surface area the photoelectrochemical activity of pristine g-C_3N_4 photoelectrochemical materials is still limited [73]. Therefore, to increase photocurrent intensity and improve the sensitivity of such PEC sensors, novel methods, such as coupling g-C_3N_4 with other semiconductor materials (Bi_2MoO_6) [74] and changing the morphology and structure of pristine g-C_3N_4 [73], have been adopted. Subsequently, the modified ionothermal method was used to improve the g-C_3N_4-based electrode and prepare 3D branched crystalline carbon nitride with 1D nanoneeds using pristine g-C_3N_4 material [75]. The PEC sensor showed a good linear detection range of 1–100 nmol/L, the LOD reached 0.38 nmol/L, and high selective sensitivity to Cu^{2+}.

3.1.3. Other PEC sensors for detection of Cu^{2+}

In addition to the CdS-based and g-C_3N_4-based PEC sensors, many other unique and novel PEC Cu^{2+}sensors that utilize various photoelectrochemical active materials have been proposed. For example, the CdTe quantum dots (QDs) was developed due to the

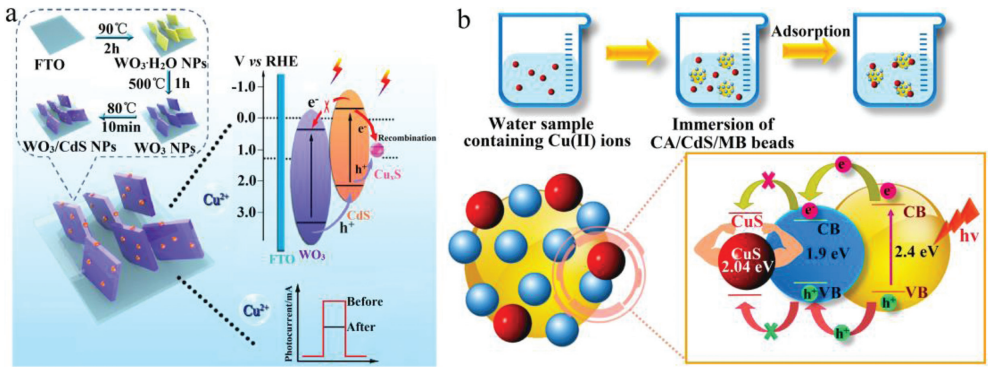

Fig. 2. (a) Schematic diagram of the WO_3/CdS composite films. Copied with permission [39]. Copyright 2019, American Chemical Society. (b) Adsorption of Cu^{2+} on the surface of CA/CdS-2/MB beads. Copied with permission [70]. Copyright 2019, Springer.

resistance of the QDs to excellent light absorption properties, photobleaching, and high efficiency of charge separation [28]. In such a PEC sensor, when the electrode is exposed to Cu^{2+}-containing solutions, a CdTe-Cu_2Te heterostructure film is formed on the electrode *in-situ*. The generated Cu_2Te particles prevent the photogenerated electrons of CdTe QDs from transferring to the electrolyte at pH 7.0, resulting in photocurrent quenching; the sensor showed a good linear relationship between photocurrent and Cu^{2+} concentration in the range of 1 nmol/L ~ 10 μmol/L and the LOD reached 0.4 nmol/L [28]. Apart from CdTe QDs, graphitic carbon nitride QDs (g-CNQDs) has also been used to prepare the photoelectrochemical sensitive materials of PEC sensors for the detection of Cu^{2+} [74].

A PEC Cu^{2+} sensor with Ni/Co_3O_4/MnO_2/chitosan heterostructure film-coated electrode was developed [76]. The sensor showed good selectivity because the energy barrier at the interface of heterostructure was formed by p-type Co_3O_4 and n-type MnO_2 (none of other substances can cause any interference above 30% for detection of Cu^{2+} ions); the sensor also showed a large detection range of 0–6500 nmol/L and a low LOD of 6.9 nmol/L. Similarly, Hammami *et al.* also constructed a PEC Cu^{2+} sensor based on the MnO_2-graphene oxide heterojunction photosensitive material [77].

Similarly, various other PEC Cu^{2+} sensors have been reported for the detection of Cu^{2+} ions. Wang *et al.* proposed a PEC Cu^{2+}sensor by using BiOI and gold nanoparticles nanohybrids [78]. Jiang *et al.* electrodeposited PbSe, PbTe, and PbS films on ITO to prepare the PEC Cu^{2+} sensors and discovered that the PbSe/ITO electrode showed the highest stable and repeatable photocurrent, that is, the PbSe/ITO PEC sensor exhibited the best sensitivity and stability [79].

3.2. Detection of Cr^{6+}

There are two common and stable oxidation states of chromium: Cr^{3+} and Cr^{6+}. Cr^{3+} is an essential micronutrient element and plays an important role in regulating glucose metabolism in humans [80]. Cr^{3+} is also a basic tanning agent and widely used in the leather, electroplating, printing, and chemical industries. However, Cr^{3+} can lead to genotoxic effects in humans, especially DNA damage and oxidative stress [80]. Furthermore, Cr^{6+} and its compounds are commonly applied in chromium smelting, chromate production, stainless steel welding, and chrome pigment production. However, Cr^{6+} is highly toxic and its compounds have been classified as Group I human carcinogens by the International Agency for Research on Cancer since 1990 [81]. Importantly, both Cr^{3+} and Cr^{6+} are widely used and have contaminated many water bodies globally [82]. The drinking-water quality guidelines of the WHO (1993) recommend that the chromium content must be limited to 0.96 μmol/L. Therefore, there is an urgent need to monitor the presence of chromium ions in water.

3.2.1. TiO_2-based PEC sensors for detection of Cr^{6+}

Numerous TiO_2-based PEC sensors have been developed for the detection of metal ions [23,61,62,83], and the first such PEC sensor for the detection of Cr^{6+} ions was reported by Li *et al.* in 2013 [30]. TiO_2 was preferred as it shows good stability, large specific surface area, and controllable morphology. To improve the sensitivity and detection range, improved TiO_2 composite coating materials were investigated. For example, Dashtian *et al.* fabricated a PEC Cr^{6+} sensor with Ti/TiO_2-$Pb_5S_2I_6$-polydopamine electrodes based on Ti foil [23]. The PEC sensor showed high sensitivity (1.9 μA L μmol^{-1}), good LOD (3 nmol/L), and wide linear range (0.01–80 μmol/L) to Cr^{6+} concentration in 0.1 mol/L deoxygenated Tris-HCl (pH 5) buffer containing 0.01 mol/L triethanolamine (TEA). To further improve sensitivity, Moakhar *et al.* proposed a Cr^{6+} PEC sensor with Au-TiO_2-coated FTO electrodes [83]. The sensor showed high selectivity, good sensitivity of 13.94 μA L μmol^{-1}, low relative standard deviation of 1.5%, and good LOD of 6 nmol/L in the Cr^{6+} concentration range of 0.01–50 μmol/L.

Furthermore, flexible substrates have also been utilized as response electrodes. Liu *et al.* fabricated a PEC Cr^{6+} sensor by using nano-particle TiO_2/graphene/gold electrode and graphene/gold/polyolefin composite flexible film that replaced FTO/ITO as substrate [61]. In another study, they replaced the polyolefin substrate with SiO_2/Si substrate and developed another PEC Cr^{6+} sensor [62]. The PEC sensors showed the sensitivity of 1.27 nA L $nmol^{-1}$ for the detection of Cr^{6+} ions.

3.2.2. Other PEC sensors for detection of Cr^{6+}

Although most PEC sensors for Cr^{6+} are based on TiO_2 and g-C_3N_4 sensitive materials and the sensing mechanism is based on the reduction of Cr^{6+} [83], TiO_2 and g-C_3N_4 belong to n-type semiconductors and are more prone to oxidation reaction. Therefore, PEC sensors based on p-type semiconductor are more suitable for the detection of Cr^{6+}because p-type semiconductors make it easy to trigger the reduction reaction [84]. Wang *et al.* constructed a PEC sensor by using p-type semiconductor PbS-coated ITO electrode [84]. The LOD reached 10 pmol/L and the linear range was 0.02 nmol/L~2 μmol/L. Furthermore, bismuth-system oxides have also attracted considerable attention for PEC Cr^{6+}sensors because of their abundance, low toxicity, low cost, and good optical and electrical properties [85]. The bismuth-system oxides used for Cr^{6+} PEC detection mainly include BiOX (X = Cl, I, Br) [55,86,87], $BiVO_4$ (Fig. 3a, I) [56,59], $BiPO_4$ [87], *etc.* Among them, p-type BiOI with strong visible-light absorption ability is a good choice PEC-sensor-based detection of Cr^{6+} ions [29]. For example, Li *et al.* fabricated a Cr^{6+} PEC sensor by using Bi-modified $BiPO_4$/BiOI composite film-coated ITO electrode [87], and the PEC sensor showed a good linear relationship between photocurrent and Cr^{6+} concentration in the range of 0.5–180 μmol/L with LOD of 0.3 μmol/L.

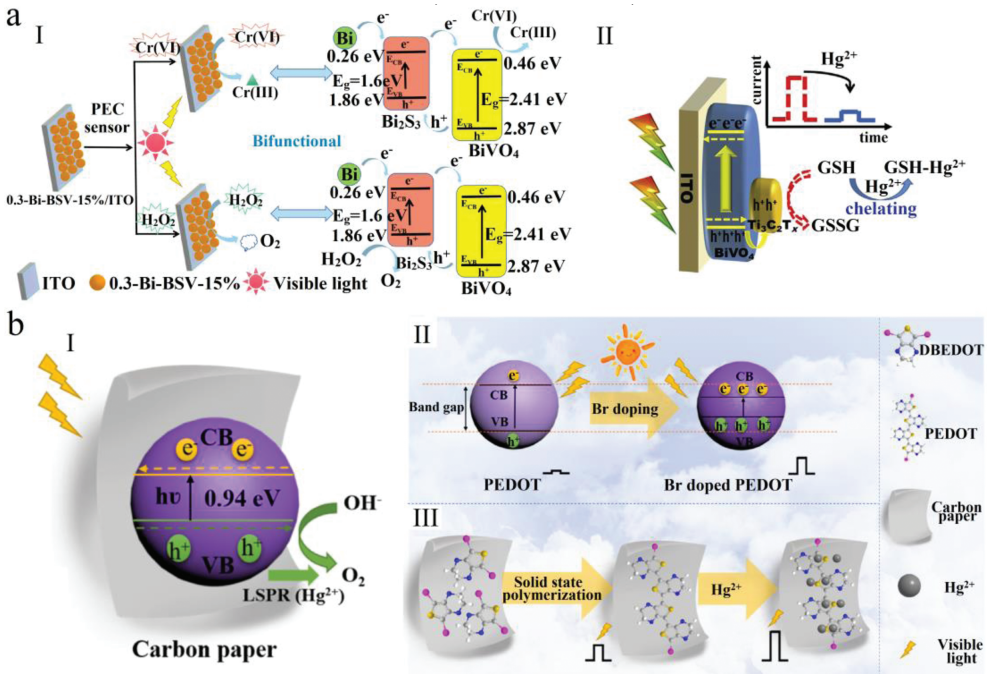

Fig. 3. (a) (I) PEC mechanism of 0.3-Bi-BSV-15% for detecting Cr^{6+}. Copied with permission [56]. Copyright 2022, Elsevier. (II) Mechanism of Hg^{2+} sensing. Copied with permission [99]. Copyright 2020, Elsevier. (b) Schematic illustration of PEDOT PEC sensor for detecting of Hg^{2+}. Copied with permission [101]. Copyright 2021, Elsevier.

3.3. Detection of Hg^{2+}

Hg^{2+} is considered to be one of the most toxic heavy metal pollutant in food, water, and biosphere [88]. Excessive Hg^{2+} accumulation in human body leads to headache, impaired hearing, and even damage to brain and central nervous system [16,89]. The United States Environmental Protection Agency (EPA 2001) specifies that the maximum level of Hg^{2+} in drinkable water is 10 nmol/L. Therefore, there is an urgent need for fast and reliable sensors that can determine even trace Hg^{2+} concentrations in water in real-time.

3.3.1. CdS-based PEC sensors for detection of Hg^{2+}

Although CdS is an important sensing material in PEC sensors, it has high carrier recombination rate and no selective sensitivity to metal ions. Thus, to selectively detect Hg^{2+} ions in water, CdS-based composites were developed [90]. For example, Zhang *et al.* developed a hollow CoS_x@CdS-modified ITO electrode to fabricate a PEC Hg^{2+}sensor [90]; the sensor showed a high selective sensitivity to Hg^{2+}, a good linear response for Hg^{2+} concentration in the range of 0.01–1000 nmol/L, and a good LOD at 2 pmol/L. Furthermore, Li *et al.* created a g-C_3N_4@CdS composite-coated FTO electrode and prepared a PEC Hg^{2+}sensor [91]. However, when the electrolyte includes Hg^{2+} ions, they will be selectively absorbed on the surface of the coating to inhibit exciton formation and photoelectron transmission, thereby decreasing the photocurrent.

3.3.2. ZnS-based PEC sensors for detection of Hg^{2+}

For PEC Hg^{2+}sensors, ZnS-based photoelectrochemical materials coated ITO electrodes have also been developed [52,92]. When the ZnS-based PEC sensors come in contact with a Hg^{2+}-containing solution, p-type semiconductor HgS is produced and coated on the surface of n-type semiconductor ZnS. The spontaneous heterojunction promotes carrier transport, resulting in evident enhancement in sensor photocurrent. Therefore, PEC sensors with ZnS-based ITO mediated electrodes can be used to quantitatively detect Hg^{2+} concentration. For example, the PEC sensors for Hg^{2+} detection were developed using an ITO electrode based on ZnS QDs capped with Cysteine and mercaptoacetic acid, respectively [92]. To improve the photocurrent response and LOD, a PEC sensor with ZnS@Ag_2S-modified electrode was created as the cocatalyst of Ag_2S QDs can effectively promote the separation of carriers in ZnS [52], thereby increasing the sensitivity of the sensor. The improved ZnS@Ag_2S-based PEC Hg^{2+} sensor showed a good LOD at 1 pmol/L.

3.3.3. TiO_2-based PEC sensors for detection of Hg^{2+}

Although TiO_2-based PEC sensors have been used to detect Cr^{6+} ions [23], they have also been developed to detect Hg^{2+} ions. To improve the performance of the PEC Hg^{2+} sensors, FTO/TiO_2/3-aminopropyltriethoxysilane (APTES)/N3 electrode was developed [93]; the photocurrent response of the sensor was relatively better because the N3-Hg^{2+} complex was formed by the presence of Hg^{2+}. The measurement range and LOD of the sensor were 0.5–50 μmol/L and 0.13 nmol/L, respectively. Furthermore, Wu *et al.* designed a PEC sensor with FTO/Ru-1/TiO_2 electrode [94]. The Ru-1 was composed of two thiocyanate ligands and Ru(II) bipyridyl complex; the photocurrent of the sensor decreased linearly with increasing of Hg^{2+} concentration over the range of 0.005–500 nmol/L and 500–5×10^6 nmol/L, and LOD of the sensor reached 5×10^{-3} nmol/L due to the specific interaction between Hg^{2+} and thiocyanate ligands.

3.3.4. Other PEC sensors for detection of Hg^{2+}

Although most PEC Hg^{2+} sensors are based on RS, CdS, ZnS, and TiO_2 composites, PEC sensors based on other sensitive materials also show good performance for the detection of Hg^{2+}. For example, Zhang *et al.* designed a PEC sensor with Ag@Ag_2S-modified ITO conductive glass [95]. Ag was deposited on the surface of Ag_2S QDs with bead-chain-like nanostructures to produce the surface plasmon resonance effect and accelerate the separation of photo-induced charges, thereby increasing the sensitivity of the PEC Hg^{2+} sensor. Importantly, the prepared PEC sensor also showed good Hg^{2+} selectivity. Furthermore, the localized surface plasmonic resonance (LSPR) effect has been explored as a means to increase the sensitivity of PEC Hg^{2+} sensors. For example, WO_3/Au nanocomposite-coated ITO electrodes were developed to increase

the sensitivity of the PEC Hg^{2+} sensors through the LSPR effect of Au [96].

In practice, novel Hg^{2+} sensitive electrodes for the preparation of PEC sensors are being continuously developed. Examples include PEC Hg^{2+} sensors with electrodes based on NiOOH-functionalized n-silicon [97], Fe^{3+}/ZnO-Ag [98], $BiVO_4/Ti_3C_2T_X$ (Fig. 3a, II) [99], and Bi_2MoO_6/CuS [100] coatings. Recently, a novel sensor with Br-doped poly(3,4-ethylenedioxythiophene) (PEDOT)-modified carbon paper was reported (Fig. 3b) [101]. The dopant of Br ions in PEDOT decreases the band gap of PEDOT; Br ions in PEDOT layer act as shuttles, promote more electron-hole separation, and greatly enhance the photocurrent intensity of the sensor. When the Br/PEDOT-based PEC sensor comes in contact with a Hg^{2+}-containing solution, the photocurrent is significantly enhanced due to the chelation of Hg^{2+} to S and O functional groups of polythiophene. The sensor shows a good linear response in the Hg^{2+} concentration over the range of 1–450 nmol/L, LOD of 0.3 nmol/L, and selectivity to Hg^{2+}.

3.4. Detection of Pb^{2+}

Lead pollution has been a longstanding global problem as Pb^{2+} can enter the human body through inhalation, intake, as well as skin contact [102]. Human exposure to Pb^{2+} can seriously harm the brain, kidney, and nervous system, and interfere with all aspects of fetal development [103]. Due to the significant threat that Pb^{2+} contamination poses to public health, the EPA has determined that the maximum permissible amount of Pb^{2+} ions in drinking water is 70 nmol/L. Therefore, it is essential to realize accurate detection of Pb^{2+} in drinking water.

3.4.1. CdS-based PEC sensors for detection of Pb^{2+}

To detect Pb^{2+} ions, a first such PEC Pb^{2+}sensor coupled with n-type semiconductor (Cds) and G-quadruplex aptamers of Pb^{2+} was developed in 2013 [54]. To improve the selectivity of PEC Pb^{2+} sensors, Pb^{2+}-selective CdS composites were developed. For example, electrodes based on MoS_2-CdS:Mn nanocomposites [104], CdS-TiO_2 nanocomposite [105], and CdSe/CdS/ZnO [48] photoelectrochemically active materials have been developed to fabricate PEC Pb^{2+} sensors. In particular, the CdS-based PEC sensor utilizing an ITO electrode based on MoS_2-CdS:Mn nanocomposites showed the widest detection range in 5×10^{-5}–100 nmol/L, a LOD of 1.67×10^{-5} nmol/L, good selectivity to Pb^{2+}, and high repeatability [104].

3.4.2. TiO_2-based PEC sensors for detection of Pb^{2+}

Although TiO_2 photocatalysts has been widely used in PEC sensors for the detection of Cr(VI) ions [23], it has also been designed for Pb^{2+} sensing. In 2022, a Cu_2O-CuO-TiO_2 heterojunction modified electrode was designed [106]. The PEC sensor based on this electrode showed a high selectivity for Pb^{2+} among the presence of other interfering ions (Cd^{2+}, Mg^{2+}, Ca^{2+} and Cu^{2+}), low LOD of 6.8×10^{-6} nmol/L, and a linear detection range of 1×10^{-5}–1000 nmol/L.

3.4.3. ZnO-based PEC sensors for detection of Pb^{2+}

ZnO-based photoelectrochemically active materials have attracted considerable attention for application in PEC Pb^{2+} sensors thanks to their high surface volume ratio, good biocompatibility, and chemical stability [107]. For example, combinations of ZnO and CdS [48] is being developed for ZnO-based Pb^{2+} PEC sensors.

3.4.4. Other PEC sensors for detection of Pb^{2+}

Apart from CdS (TiO_2- and ZnO-)-based materials, BiOI [108], g-C_3N_4 [109], 3,4,9,10-perylene tetracarboxylic acid [110,111], nickel hexacyanoferrate [112], and porphyrin-based covalent organic framework (TAPP-COF) [113] were developed for use in the design of PEC sensors for the detection of Pb^{2+}. For example, Zhao *et al.* fabricated such a sensor based on a TAPP-COF film-coated electrode (Fig. 4a) [113]. First, the prepared TAPP-COF thin film was transferred onto a poly(ethylene terephthalate) (PET)-based ITO electrode. Subsequently, CdSe QDs coated with a SiO_2 shell (CdSe@SiO_2 QDs) were immobilized on TAPP-COF film. In the presence of Pb^{2+}, the quencher CdSe@SiO_2 QDs immediately detached from TAPP-COF film, the quenching effect caused by CdSe@SiO_2 QDs disappeared, the photocurrent increased. The sensor showed a good linear detection range of 1×10^{-5}–1000 nmol/L, low LOD of 0.012 nmol/L, and high selectivity to Pb^{2+}.

3.5. Detection of Ag^{+}

Ag^{+} is one of the trace elements found in the human body. It is widely used in jewelry, skin care products, and other commodities as trace amounts of silver are generally harmless to human health [114]. However, silver exists in nature as a heavy metal ion to form silver salt. Silver salts are toxic to humans because they can be absorbed into the human circulatory system and become deposited in various body tissues. This can lead to argyria including inhibition of the activity of the enzymes, cell apoptosis and decrease in the expression level of genes [115]. The guideline value of EPA for silver in public water supplies is 0.93 μmol/L. Hence, it is imperative to detect Ag^{+} economically and reliably.

In 2014, Li *et al.* developed the first PEC sensor with AgBr-enhanced ZnO nanorod-based electrode to detect Ag^{+} ions [34]. To improve the sensitivity and LOD of the sensor, Li *et al.* further developed another PEC sensor utilizing an ITO electrode based on yolk-shell-structured Fe_3O_4@void@TiO_2-Na^{+} particles (Fig. 4b) [116]. The prepared Fe_3O_4@void@TiO_2-Na^{+} particles were immersed in a solution containing Ag^{+}; after magnetic separation and washing process, Fe_3O_4@void@TiO_2-Ag^{+} particles were obtained through Ag^{+}-Na^{+} ion exchange. The exothermic electron injection mechanism of the *in-situ* generated nanosilver particles significantly increased the photocurrent; therefore, the proportional increment in photocurrent can be utilized to detect Ag^{+} ions. The PEC sensor showed high selectivity for Ag^{+} in 0.1 mol/L phosphate-buffered saline (pH 7.0) due to Ag^{+}-Na^{+} ion exchange and *in-situ* formation of plasma Ag nanoparticles. The PEC sensor also showed a good linear detection range of 1 pmol/L∼6 nmol/L and LOD of 0.88 pmol/L.

3.6. Detection of K^{+}

K^{+} is an important mineral that helps in maintaining the balance of fluid and electrolyte in biological systems and regulates body functions [117]. It plays an important role in many physiological functions, including cellular metabolism, glycogen and protein synthesis, and regulation of electrical action potential across cell membranes [118]. However, excessive intake of K^{+} can lead to diseases such as abnormal heart rhythm. The maximum allowable level for K^{+} ions in drinkable water defined by the WHO (2011) is 0.31 mmol/L. Hence, it is necessary to develop a reliable method for the analysis of K^{+} in water.

Qian *et al.* proposed a PEC sensor with an ITO electrode based on potassium-selective polymer dots (K-Pdots) (Fig. 5a) [35]. When the electrode was immersed in a K^{+} solution, the exposure of K^{+} to K-Pdots initiated the transport of K^{+} ions into the Pdots and their subsequent binding with the ionophores. The hydrogen ions in K-Pdots moved toward outside of K-Pdots, resulting in the deprotonation of –COOH in the K-Pdots, and thereby reducing the production of carriers at the surface of K-Pdots, causing a corresponding decrease in photocurrent. The PEC sensor showed a good

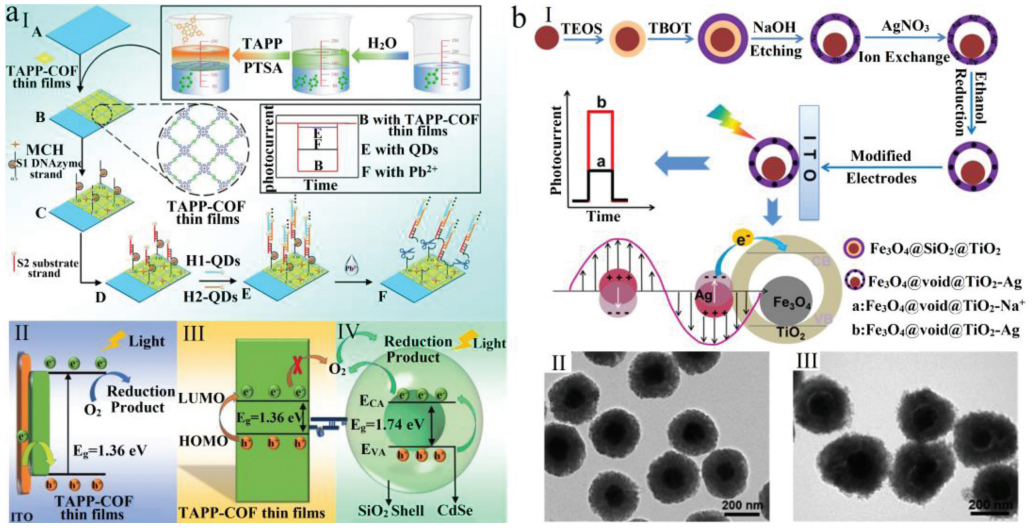

Fig. 4. (a) Fabrication procedure and sensing mechanism of the TAPP-COF thin-film-based PEC Pb^{2+} sensor for Pb^{2+}. Copied with permission [113]. Copyright 2021, American Chemical Society. (b) Schematic illustration of preparation of ITO electrode based on yolk-shell-structured Fe_3O_4@void@TiO_2-Na^+ particles (I) and images of Fe_3O_4@SiO_2@TiO_2 (II) and Fe_3O_4@void@TiO_2-Ag^+(III). Copied with permission [116]. Copyright 2020, American Chemical Society.

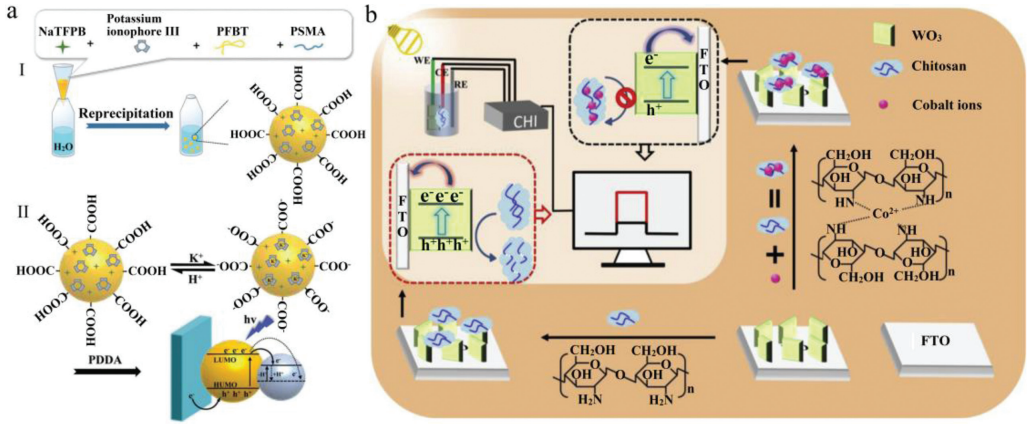

Fig. 5. (a) (I) Schematic of the preparation of K-Pdots and (II) PEC sensor with K-Pdots for the detection of K^+. Copied with permission [35]. Copyright 2021, the Royal Society of Chemistry. (b) Illustration of PEC process of CS/WO_3/FTO and its application for Co^{2+} analysis. Copied with permission [36]. Copyright 2019, Elsevier.

linear detection range of $1{\sim}1\times10^5$ nmol/L, LOD of 0.421 nmol/L, and a good selectivity to K^+.

3.7. Detection of Co^{2+}

Cobalt is an essential trace element for both prokaryotes and eukaryotes, and it occurs naturally in organic and inorganic forms [9]. Cobalt ions (Co^{2+}) play an important role in various biological processes involving a multitude of physiological functions, including the protection of nervous system, formation of red blood cells, DNA synthesis, and iron and amino acid metabolism [119]. It has been demonstrated that deficiency of Co may cause in cardiovascular, anemia, neuropsychiatric, osteomyelitis and glaucoma, and endocrine deficits [9]. However, excessive intake of cobalt can induce poisoning and has adverse effects on the health of skin, lung, and thyroid when concentration in the blood exceeds 5.09 mmol/L [120]. Therefore, it is very important to build a sensitive and reliable sensor to detect Co^{2+} in water.

The first PEC sensor to detect $Co^{2+}$was proposed by Zheng *et al.* in 2019 [36], which utilized a FTO/WO_3/Chitosan (CS) electrode. Modifying FTO/WO_3 with CS can significantly improve the visible-light absorption and the separation efficiency of photogenerated carriers, and can thus significantly improve the photocurrent due to the CS is an efficient hole scavenger. In the presence of Co^{2+}, CS can be used as a chelating agent to effectively extract Co^{2+} from water. In addition, the formation of Co-CS chelate inhibits the electron transfer from CS to the photogenerated holes of WO_3, resulting in low separation efficiency of WO_3 photogenerated carriers and subsequently decreasing the photocurrent (Fig. 5b). The aforementioned PEC sensor showed a broad linear response for Co^{2+} concentration in the range of 1–60 μmol/L, a LOD of 0.3 μmol/L, and a high selectivity for Co^{2+} in phosphate buffer (pH 6.5).

3.8. Detection of As^{5+}

Arsenic (As^{5+}) is one of the most widely distributed inorganic contaminants in the world [121]. If its intake exceeds the excretion rate, arsenic will accumulate in human organs, leading to chronic poisoning, neuritis, myelitis, *etc.* The WHO (1993) stipulates that the maximum contamination level of As^{5+} in drinking water should be limited to 0.133 μmol/L. Therefore, it is important to accurately detect As^{5+} in drinking water and food.

Recently, Fu *et al.* proposed a novel PEC sensor utilizing a $AgInS_2$/oligonucleotides/FePc based ITO electrode for detecting As^{5+} (Fig. 6a) [60]. To develop the PEC As^{5+} sensor, magnetic Co_3O_4-Fe_3O_4 cubes were prepared and then functionalized with oligonucleotides. In the presence of As^{5+}, oligonucleotides can be released and As^{5+} can be absorbed due to the strong affinity be-

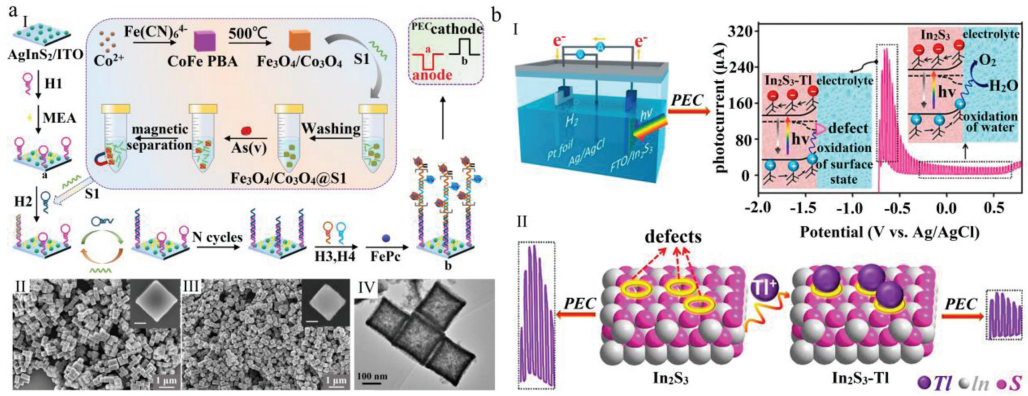

Fig. 6. (a) Schematic diagram for the PEC detection of As^{5+} (I) and images of CoFe PBA (II), Co_3O_4-Fe_3O_4 cubes (III), and Co_3O_4-Fe_3O_4 cubes (IV). Copied with permission [60]. Copyright 2022, American Chemical Society. (b) Schematic illustration of PEC system and proposed mechanism for detection of Tl^+ on the basis of surface state passivation. Copied with permission [51]. Copyright 2021, American Chemical Society.

tween As^{5+} and Co_3O_4-Fe_3O_4 cubes. Subsequently, the released oligonucleotides trigger catalytic hairpin assembly and hybridization chain reaction, forming a large number of G-quadruplex structures on the electrode. Then, phthalocyanine was captured by the G-quadruplex structures, leading to a switch in the photocurrent polarity of electrode from anode to the cathode. The PEC sensor showed a good linear detection range of $10\sim2\times10^5$ nmol/L and selectivity for As^{5+} with LOD at 1 nmol/L. However, except As^{5+}, PO_4^{3-} can also switch the polarity of photocurrent; therefore, to accurately monitor As^{5+} in water, the analyte should be pretreated to eliminate any interference from PO_4^{3-}.

3.9. Detection of Tl^+

Thallium is a very rare but widely dispersed trace element. There are two common and stable oxidation states of thallium: Tl^{3+} and Tl^+; compared to the former, monovalent thallium compounds have relatively high solubility and are toxic to organisms [122]. The toxicity of Tl^+ is higher than other heavy metals such as Hg, Pb, and Cd [123]. Moreover, it is readily transported to the environment through aqueous routes and gradually accumulates. Excessive intake of Tl^+ can easily cause esophageal cancer, liver cancer, and other diseases. The WHO (1993) has warned that the concentration of thallium in drinking water must not exceed the threshold limit of 9.8 nmol/L. Therefore, the detection of Tl^+ is of great significance for effective monitoring of the hydrosphere and human health.

Wei *et al.* reported a PEC Tl^+ sensor using a sulfide-rich In_2S_3 coated FTO electrode [51]. When the bias potential was scanned from –0.8 V to 0.8 V *vs.* Ag/AgCl, the surface state-rich In_2S_3 showed significant anodic photocurrent response. The photocurrent gradually reached a steady-state (Fig. 6b) with further increase in bias potential, and the peak value of photocurrent was approximately –0.65 V. The appearance of the peak value is caused by the direct oxidation of sulfide surface states by photogenerated holes, while the latter stable state is regarded as the consequence of water oxidation. In the presence of Tl^+, the surface sulfide will chemically combine with Tl^+, which will greatly decrease the photoactivity of sulfide and lead to the quenching of photocurrent at –0.65 V. The sensor showed a linear response for Tl^+ concentration in the range of 0.625–10 μmol/L with LOD of 0.36 μmol/L. However, when the concentrations of Co^{2+}, La^{3+}, and Cu^{2+} were 30 times higher than that of Tl^+ and the concentrations of Pb^{2+}, Hg^{2+}, and Cd^{2+} were 10 times higher than that of Tl^+, addition of ethylenediaminetetraacetic acid was required to carry out the accurate detection of Tl^+.

4. PEC sensors for non-metal ions

4.1. Detection of NO_2^-

Nitrite anions (NO_2^-) are considered a common inorganic environmental pollutant [124], and NO_2^- can react with amines to form carcinogenic nitrosamines [125]. In high doses, it is toxic and can lead to food poisoning, methemoglobinemia, and other conditions that are harmful to human health [126]. According to the regulation by WHO (2003), the maximum contaminant level for nitrite is 0.065 mmol/L in drinking water. Hence, it is necessary to develop novel approaches for accurate detection of NO_2^-.

4.1.1. TiO_2-based PEC sensors for detection of NO_2^-

Currently, TiO_2-based composites are the most commonly used photoelectrochemically active materials in PEC sensors for the detection of NO_2^-. A TiO_2-based PEC sensor was fabricated through the application of disposable screen-printed carbon substrates with TiO_2-P25 nanoparticles to detect NO_2^- [127]. To improve the selectivity and detection range of PEC NO_2^-sensors, Muthuchamy *et al.* fabricated a TiO_2-based PEC NO_2^- sensor: First, the graphene (G) was modified by using an electroconductive polymer nanosponge (EPNS) and TiO_2 nanowires (named TiO_2 (G) NW@EPNS); second, cytochrome C (Cyt C) was immobilized into TiO_2 (G) NW@EPNS (Fig. 7a) [128]. The PEC sensor showed a high selectivity for NO_2^-, a good detection range of 0.5–9000 μmol/L, a LOD of 225 μmol/L, and a rapid response (~5 s). Furthermore, to improve the LOD of the NO_2^- sensors, Gao *et al.* constructed a PEC NO_2^- sensor an FTO electrode based on CdS/TiO_2 nanocomposites (NCs) (nitrite is considered as an active oxidant under acidic conditions) (Fig. 7b) [129]. In the presence of NO_2^-, NO_2^- will trigger CdS etching reaction. With the dissolution of CdS, the photocurrent conversion efficiency of the sensor decreases sharply under visible light, resulting in a significant decrease in photocurrent response. The photocurrent of the sensor decreases linearly with an increase in the NO_2^- concentration over 1–100 μmol/L and 100–500 μmol/L and the LOD of the sensor was 0.56 μmol/L. Furthermore, the PEC sensor showed good selectivity to NO_2^-.

4.1.2. Other PEC sensors for detection of NO_2^-

Recently, Luo *et al.* reported a three-dimensional network nanocomposite composed of SnO_2 nanofibers and Au nanoparticles (NPs), and evaluated the anti-interference ability of ITO/SnO_2-AuNPs electrode (Fig. 8a) [58]. Photosensitizer $Ru(bpy)_3^{2-}$ was added into the NO_2^- sensitive electrode to improve the performance of the detection system. Under illumination, Ru^{2+} is excited

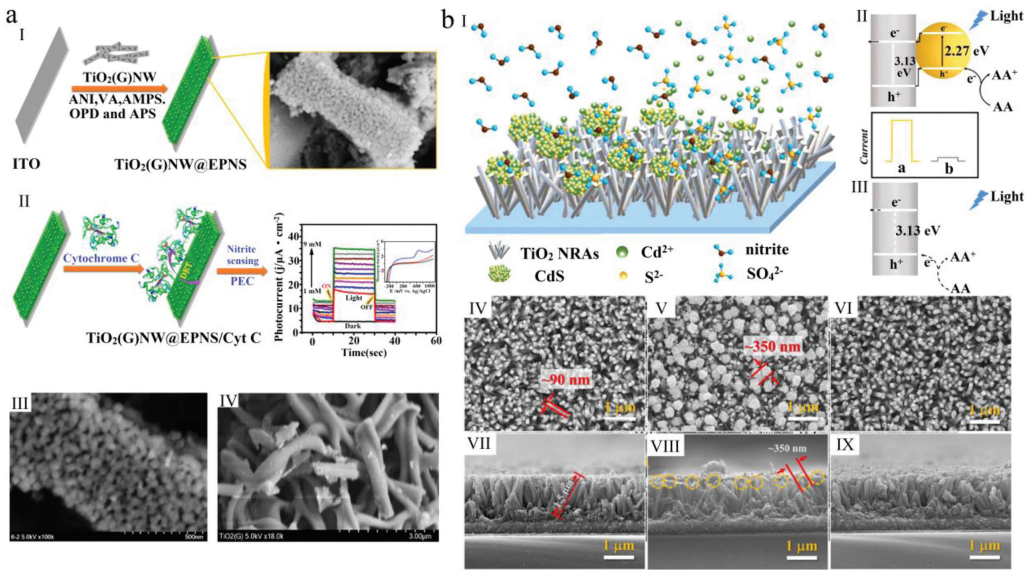

Fig. 7. (a) Preparation of electroconductive polymer nanosponges coated TiO_2(G) (I) and TiO_2(G) NW@EPNS/Cyt C biosensor (II) as well as images of TiO_2(G) NW@EPNS (III) and pristine TiO_2 NW (IV). Copied with permission [128]. Copyright 2017, Elsevier. (b) Schematic illustration of the CdS Etching Process on the CdS/TiO_2 NC-Based PEC Sensor (I) and the charge-transfer process (II and III), images of the top view (IV, V) and horizontal view (VII–IX) of TiO_2 NRAs (IV), CdS/TiO_2 NC (V), etched CdS/TiO_2 NC (VI) samples, respectively. Copied with permission [129].Copyright 2020, American Chemical Society.

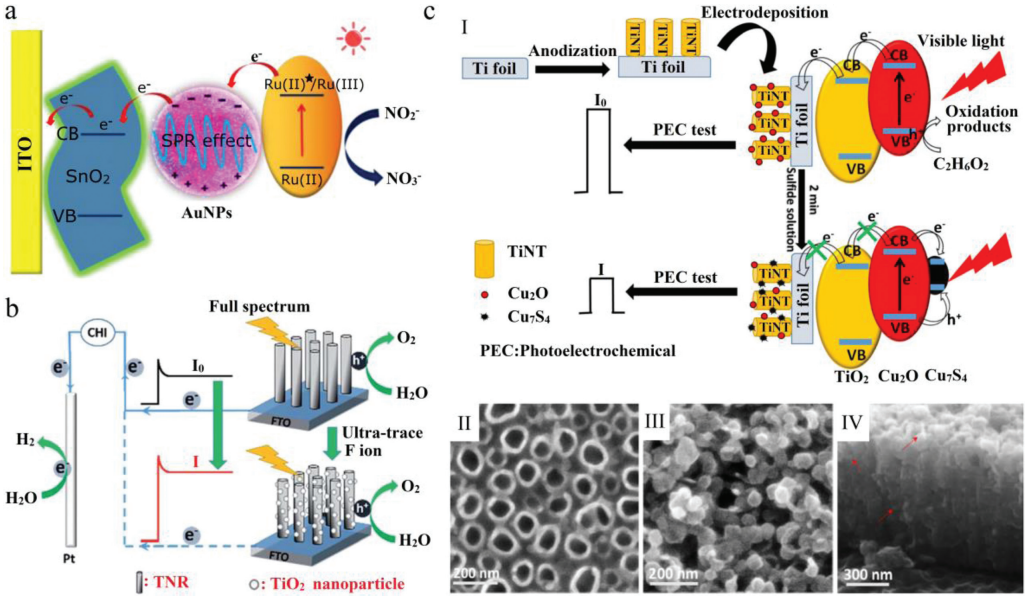

Fig. 8. (a) The transfer of the photogenerated electrons and the possible mechanism of sensing NO_2^-. Copied with permission [58]. Copyright 2020, Elsevier. (b) Schematic illustration of the photoelectrochemical probe for the detection of F^- ion. Copied with permission [131]. Copyright 2019, The Royal Society of Chemistry. (c) Schematic illustration of the photoelectrochemical sensor for the detection of sulfide (I) and SEM images of the TiNTs (II) and Cu_2O/TiNT-80 (III, IV). Copied with permission [47]. Copyright 2017, Springer.

into unstable Ru^{2+*} and rapidly transfers electrons to adjacent conductor of AuNPs or SnO_2 nanofibers, turning itself into Ru^{3+}. Simultaneously, the hot electrons in AuNPs are also excited to the surface plasma state. The electrons flowing into AuNPs are transferred to the CB of SnO_2 due to the matched energy level. Subsequently, the electrons are guided to the external circuit to generate a photocurrent response. In the presence of NO_2^-, Ru^{3+} ions react with NO_2^- ions to form NO_3^- and Ru^{2+} ions. This means that the presence of NO_2^- restores the oxidative state of ruthenium and improves the PEC response, so as to establish the relationship between photocurrent intensity and NO_2^- concentration. The photocurrent of the PEC sensor increases linearly with NO_2^- concentrations ranging over $10^{-9} \sim 10^{-5}$ mol/L with a LOD of 48 nmol/L. Furthermore, the PEC sensor showed good anti-interference performance.

4.2. Detection of F^-

Fluorine is generally beneficial to human health and is commonly used for the prevention of dental caries and treatment of osteoporosis, obesity disorders, and cardiovascular diseases [130]. However, excess fluoride intake can result in numerous health problems, such as dental fluorosis and skeletal fluorosis in children, impaired thyroid, chronic kidney disease, and endocrine system

Table 1
PEC sensors for the detection of ions.

Analyte	Electrode/substrate	Measurement principle	Linear range (nmol/L)	LOD (nmol/L)	Guideline values (nmol/L)	Refs.
Cu^{2+}	FTO/CdS/Ti_3C_2	Decrease	$0.1 \sim 1 \times 10^4$	0.05	2×10^4	[67]
Cr^{6+}	ITO/PbS QDs	Increase	$0.02 \sim 2 \times 10^3$	0.01	960	[84]
Hg^{2+}	FTO/Ru-1/TiO_2	Decrease	$0.005 \sim 5 \times 10^6$	0.005	10	[94]
Pb^{2+}	ITO/Cu_2O-CuO-TiO_2	Increase	$1 \times 10^{-5} \sim 1 \times 10^3$	6.8×10^{-6}	70	[106]
Ag^{+}	ITO/Fe_3O_4@void@TiO_2-Na^{+}	Increase	$1 \times 10^{-3} \sim 6$	8.8×10^{-4}	930	[116]
K^{+}	ITO/K-Pdots	Decrease	$1 \sim 1 \times 10^5$	0.421	3.1×10^5	[35]
Co^{2+}	FTO/WO_3/CS	Decrease	$1 \times 10^3 \sim 6 \times 10^4$	300	1.7×10^3	[36]
As^{5+}	ITO/$AgInS_2$/H1/MEA/H2/H3-H4/FePc	Polarity-switchable	$10 \sim 2 \times 10^5$	1	133	[60]
Tl^{+}	FTO/In_2S_3	Increase	$625 \sim 1 \times 10^4$	360	9.8	[51]
NO_2^{-}	ITO/SnO_2-Au-Ru(bpy)$_3^{2-}$	Increase	$1 \sim 1 \times 10^4$	0.48	6.5×10^4	[58]
F^{-}	FTO/TiO_2	Increase	$0.05 \sim 1000$	0.03	7.9×10^4	[131]
S^{2-}	Ti/TiO_2/Cu_2O	Decrease	$1 \times 10^3 \sim 3 \times 10^5$	600	1.6×10^4	[47]

function or developmental neurotoxicity [130]. Unfortunately, fluoride compounds are widely present in the environment because of natural and anthropogenic activities, resulting in the accumulation of F^- in the soil, air, water, and in humans as well. Particularly, endemic fluorosis is present in many countries, including Africa and Asia due to drinking water contaminated with fluoride [130]. Therefore, keeping the F^- content in drinking water below the accepted thresholds is very important for human health, and the WHO (2010) guideline value for F^- concentration in drinking water is set at 0.079 mmol/L. Thus, to effectively protect the impact of excess F^- on human health, it is necessary to accurately detect the F^- concentration.

A PEC F^- sensor utilizing TiO_2 nanorod array (TNRs)-based FTO electrode was first proposed by Su *et al.* in 2019 [131]. When the TNR-based PEC sensor comes in contact with an F^--containing solution, F^- ions trigger an etching reaction on the surface of the TNRs, resulting in more surface-active sites and smaller electron transfer resistance, which increases photocurrent density (Fig. 8b). The PEC F^- sensor shows a good linear response to F^- ion concentration over the range of 0.05–1000 nmol/L along with an ultratrace LOD of 0.03 nmol/L and high selectivity for F^- in 0.1 mol/L Na_2SO_4 among interfering ions.

4.3. Detection of S^{2-}

Sulfide (S^{2-}), as a toxic pollutant in wastewater, is of great concern for the environment [132]. High concentrations of S^{2-} can cause multiple serious health problems such as unconsciousness or even permanent brain damage [133]. In addition, it can get further protonated and converted to more toxic gaseous such as HS^- and H_2S under acidic conditions. In general, the amount of sulfide in the solution is expressed as the sum of dissolved H_2S, HS^-, and S^{2-}, and it reaches equilibrium relying on the pH of the solution [134]. To assure safe drinking water, the maximum level of S^{2-} in drinking water prescribed the WHO (2004) is 0.016 mmol/L. Thus, there is an imminent need to develop highly selective sensors to detect S^{2-} in water.

In 2001, Shchukin *et al.* first proposed a PEC sensor with CdO electrode to detect S^{2-} ions [135]. Subsequently, Su *et al.* developed another PEC S^{2-} sensor by utilizing a Cu_2O/TiO_2 nanotube (TiNTs) based Ti foil [47]. When the Cu_2O/TiNT electrode is suspended in the sulfide solution, Cu_7S_4 is formed on the surface of electrode, and the photogenerated carriers from Cu_2O nanoparticles are transferred to Cu_7S_4 and rapidly combine with Cu_7S_4, resulting in a decrease in photocurrent (Fig. 8c). The photocurrent of the sensor decreased linearly over an S^{2-} concentration range of 1–300 μmol/L with a LOD of 0.6 μmol/L. Particularly, the sensor showed a high selectivity for sulfide in 0.1 mol/L Na_2SO_4 solution containing interference ions.

5. Conclusion and future prospects

In this review, we have systematically outlined the latest important developments regarding PEC ion sensors in the literature since January 2017. Importantly, the composition (photoelectrochemically active materials and conductive substrates), measurement principle (electronic transfer, chemical reaction, and photocurrent variation characteristics), and performance of the sensors for detecting trace metal and non-metal ions are summarized according to ion species.

Although these extensive studies have significantly advanced the development of PEC ion sensors, detectable ion species may have to be expanded and the performance of some sensors needs to be further improved, because our purpose is to ensure that the tested drinking water is safe for humans and we must be able to accurately detect trace ions in water. Clearly, the performance of the PEC sensors for K^+, Co^{2+}, As^{5+}, Tl^+, NO_2^-, F^-, and S^{2-} should be further enhanced. Particularly, the LOD values of PEC sensors for Co^{2+}, Tl^+ and S^{2-} need to be further improved (Table 1). Besides, the stability, repeatability, portability, multiple detection and anti-interference ability (temperature, pH value, microorganism, *etc.*) of PEC ion sensors still need to be improved, which are the main obstacles that hinder their development into commercial products for practical applications. We understand that the LOD, detection range, and sensitivity of PEC sensors are controlled by the intensity of the generated photocurrent. Although the photocurrent of the PEC sensors is controlled by many factors (photoreactor structure, conductive substrate, electrolyte, photoelectrochemically active materials, and so on), the ion sensing material is the most important factor affecting the photocurrent because it determines the light absorption, photoelectric conversion, electron and hole recombination, electron transfer, and reaction between the active material with the detection target ions. Furthermore, the performance of these materials is controlled by their band structure, work function, molecular and morphology structures, and specific surface area. Therefore, to improve the LOD, detection range, and sensitivity of PEC sensors, more advanced photoelectrochemical active materials should be developed or imported from other PEC research applications such as water splitting, wastewater treatment, and reduction of carbon dioxide.

The selectivity of PEC ion sensors has been investigated in the presence of a series of interference ions. The results highlight that most of the developed PEC ion sensors have good selectivity for target ions, which means that these sensors have a certain anti-interference ability. In particular, PEC DNAzyme biosensors show high selectivity and specificity for metal ions because DNAzyme molecules can strongly and selectively bind metal ions. However, when PEC ion sensors are applied to monitor ions in surface and groundwater sources, especially polluted water, it is not enough

to only consider the influence of other interfering ions. Other interfering factors such as temperature, pH, and common pollutants (such as microorganisms and suspended particles) may affect the response of the PEC ion sensors. Therefore, to improve the anti-interference ability of these sensors and make them more flexible in practice, it is necessary to further enhance the anti-interference ability of the PEC ion sensors to avoid the influence of temperature, pH, microorganisms, suspended particles, *etc.*

In addition to the importance of sensitivity, LOD, detection range, and anti-interference ability of the PEC ion sensors, their repeatability and lifetime are also key factors that determine their applicability in the real world. The relative standard deviations can judge the stability of the PEC ion sensor. Although the relative standard deviations of some PEC ion sensors have been tested and showed a good result, they still face certain critical issues that need to be addressed. Moreover, the photo-corrosion of photoelectrochemically active materials and their separation from the conductive substrate surface can lead to poor charge-transfer properties and rapid electron-hole recombination, thereby decreasing the photoelectric conversion efficiency and dropping the stability and repeatability of the PEC ion sensors. Furthermore, in the process of reuse and continuous detection of PEC ion sensors, the accumulation of products or non-target ions on the electrode surface will hinder the absorption of light by the photoelectrochemically active materials and block the active sites on the electrode surface as well as hinder the reaction between the target analyte and active material, thereby leading to material deactivation and reduced service life. The performance degradation gets worse when the photo-corrosion and accumulation of reaction products and non-target ions occur simultaneously on the electrode surface. For example, in the PEC Cu^{2+} sensor, which comprises a CdS-coated ITO electrode, Cd^{2+} will be produced when CdS is subjected to photo-corrosion or CdS undergoes displacement reaction with target ions to produce other substances (such as Cu_XS). On the contrary, wastewater, even domestic water, contains a large amount of ions; thus, attempts to detect trace amounts of Cu^{2+} or Zn^{2+} ions (10^{-6} mol/L) in such water will lead to marked decline in the photocatalytic activity due to the presence of metal ions that will continuously quench the photogenerated electrons and holes. To overcome the above problems, first, a protective layer (such as Ag_3PO_4) should be deposited on the surface of the photoelectrochemically active material to prevent photo-corrosion and detachment of the active material, inhibit the recombination of carriers, and enhance the charge transmission. Second, the addition of sacrificial agents in the electrolyte can also inhibit photo-corrosion; for example, when CdS is used as a photoelectrochemically active material, adding Na_2SO_3 and Na_2S as sacrificial agent in the solution can effectively inhibit the photo-corrosion. Third, to form a strong interphase between the photoelectrochemically active material and conductive substrate, an appropriate crosslinking agent should be developed and adopted to produce a strong bond between the active material and substrate, thereby enhancing the sustainability and repeatability of PEC sensors. Fourth, the strategy of self-sensitization effect, in which the heavy metal ions convert into the metal sulfides or even form a heterojunction structure with the prepared photoelectrochemically active materials, could be positively utilized to enhance the stability and photocurrent of the PEC ion sensors.

Although extensive research has been carried out to produce PEC sensors with high sensitivity, wide detection range, good LOD, and high repeatability, there are still some inherent challenges for multi-parameter online ion detection in real time. More suitable synthetic strategies for the design of PEC ion sensors are needed to address these challenges. In particular, coupling of PEC system, microfluidics, and lab-on-a-chip may be an effective method to eliminate the water sample collection process and directly realize real-time online detection of surface- and groundwater sources. Furthermore, the distribution of a variety of different sensitive materials on a conductive substrate may build different photocurrent generated to response of different ions, which may be a new research path that can allow PEC sensors to achieve simultaneous detection of multiple ions.

Declaration of competing interest

There are no conflicts to declare.

Acknowledgments

The authors acknowledge financial support from the National Natural Science Foundation of China (NSFC, Nos. 52176178, 51876018), Innovation Research Group of Universities in Chongqing (No. CXQT21035), Scientific and Technological Research Program of Chongqing Municipal Education Commission of China (No. KJZD-M202201101), Chongqing Postgraduate Innovation Project (No. CYS22645).

References

[1] T. Tao, K. Xin, Nature 511 (2014) 527–528.
[2] S. Bolisetty, M. Peydayesh, R. Mezzenga, Chem. Soc. Rev. 48 (2019) 463–487.
[3] G.L. Sun, E. Reynolds, A.M. Belcher, Nat. Sustain. 3 (2020) 303–311.
[4] M. Valls, S. Atrian, V. de Lorenzo, L.A. Fernández, Nat. Biotechnol. 18 (2000) 661–665.
[5] H. Han, H.J. Nakaoka, L. Hofmann, et al., Nat. Cell Biol. 24 (2022) 74–87.
[6] P. Tian, C. Feng, T.P. Loh, Nat. Commun. 6 (2015) 1–7.
[7] A.K. Sonkar, A. Rai, K. Tripathi, et al., Sens. Actuators B: Chem. 327 (2021) 129011.
[8] R. Kumar, H. Münstedt, Biomaterials 26 (2005) 2081–2088.
[9] B. Ke, L. Ma, T. Kang, et al., Anal. Chem. 90 (2018) 4946–4950.
[10] H. Kabir, A.K. Gupta, S. Tripathy, Crit. Rev. Environ. Sci. Technol. 50 (2020) 1116–1193.
[11] V.A. Luyckx, Z. Al-Aly, A.K. Bello, et al., Nat. Rev. Nephrol. 17 (2021) 15–32.
[12] Q. Bao, G. Li, Z. Yang, et al., Chin. Chem. Lett. 31 (2020) 2752–2756.
[13] A. Boetius, Nat. Rev. Microbiol. 17 (2019) 331–332.
[14] J.V. Vaghasiya, C.C. Mayorga-Martinez, S. Matějková, M. Pumera, Nat. Commun. 13 (2022) 1–10.
[15] L. Song, S. Jing, Y. Qiu, F. Liu, A. Li, Chin. Chem. Lett. 34 (2023) 107180.
[16] L. Jiao, N. Zhong, X. Zhao, et al., TrAC Trends Anal. Chem. 127 (2020) 115892.
[17] Q. Zheng, X. Teng, Q. Li, et al., Sens. Actuators B: Chem. 346 (2021) 130468.
[18] H. Karimi-Maleh, Y. Orooji, F. Karimi, et al., Biosens. Bioelectron. 184 (2021) 113252.
[19] M. Cuartero, Sens. Actuators B: Chem. 334 (2021) 129635.
[20] Z. Zhou, S. Chen, Y. Huang, et al., Biosens. Bioelectron. 198 (2022) 113858.
[21] N. Zhong, Z. Wang, M. Chen, et al., Sens. Actuators B: Chem. 254 (2018) 133–142.
[22] Y. Han, R. Zhang, C. Dong, F. Cheng, Y. Guo, Biosens. Bioelectron. 142 (2019) 111529.
[23] K. Dashtian, M. Ghaedi, S. Hajati, Biosens. Bioelectron. 132 (2019) 105–114.
[24] W. Zhao, J. Xu, H. Chen, Biosens. Bioelectron. 92 (2017) 294–304.
[25] Y. Zhao, H. Luo, Q. Ge, et al., Sens. Actuators B: Chem. 336 (2021) 129750.
[26] Z. Hu, Y. Xu, H. Wang, G. Fan, X. Luo, Chin. Chem. Lett. 33 (2022) 4750–4755.
[27] Q. Chen, C. Yuan, C. Zhai, Chin. Chem. Lett. 33 (2022) 983–986.
[28] J. Li, F. Mo, L. Guo, et al., Sens. Actuators B: Chem. 328 (2021) 129032.
[29] H. Wang, H. Ye, B. Zhang, F. Zhao, B. Zeng, J. Mater. Chem. A 5 (2017) 10599–10608.
[30] H. Li, J. Li, W. Wang, et al., Analyst 138 (2013) 1167–1173.
[31] J. Chamier, J. Leaner, A.M. Crouch, Anal. Chim. Acta 661 (2010) 91–96.
[32] X. Zhang, S. Li, X. Jin, S. Zhang, Chem. Commun. 47 (2011) 4929–4931.
[33] Y. Liang, B. Kong, A. Zhu, Z. Wang, Y. Tian, Chem. Commun. 48 (2012) 245–247.
[34] J. Li, W. Tu, H. Li, J. Bao, Z. Dai, Chem. Commun. 50 (2014) 2108–2110.
[35] Y. Qian, Y. Li, Y. Qin, D. Jiang, H. Chen, Analyst 146 (2021) 450–453.
[36] C. Zheng, B. Li, C. Hong, A. Peng, X. Chen, J. Electroanal. Chem. 851 (2019) 113470.
[37] F. Huang, F. Pu, X. Lu, et al., Sens. Actuators B: Chem. 183 (2013) 601–607.
[38] J. Liu, Y. Liu, W. Wang, et al., Sci. China Chem. 62 (2019) 1725–1731.
[39] J. Wang, Y. Pan, L. Jiang, et al., ACS Appl. Mater. Interfaces 11 (2019) 37541–37549.
[40] W. Zhao, J. Xu, H. Chen, Analyst 141 (2016) 4262–4271.
[41] B. Peng, L. Tang, G. Zeng, et al., Curr. Anal. Chem. 14 (2018) 4–12.
[42] W. Zhao, J. Wang, Y. Zhu, J. Xu, H. Chen, Anal. Chem. 87 (2015) 9520–9531.
[43] Z. Qiu, D. Tang, J. Mater. Chem. B 8 (2020) 2541–2561.
[44] H. Zhou, J. Liu, S. Zhang, TrAC Trends Anal. Chem. 67 (2015) 56–73.
[45] G. Wang, J. Xu, H. Chen, Sci. China Ser. B: Chem. 52 (2009) 1789–1800.
[46] G. Wang, J. Xu, H. Chen, Nanoscale 2 (2010) 1112–1114.
[47] Y. Su, S. Yang, W. Liu, et al., Microchim. Acta 184 (2017) 4065–4072.

[48] J. Cao, X. Liao, Y. Wang, Y. Liu, J. Electroanal. Chem. 880 (2021) 114828.
[49] D.M. Han, L.Y. Jiang, W.Y. Tang, et al., J. Electroanal. Chem. 778 (2016) 148–151.
[50] J. Chen, G.C. Zhao, Y. Wei, D. Feng, H. Zhang, Electrochim. Acta 370 (2021) 137736.
[51] Q.Y. Wei, Y.F. Ji, Y.Y. Geng, et al., ACS Appl. Electron. 3 (2021) 2490–2496.
[52] L. Zhang, P. Li, L. Feng, et al., J. Hazard. Mater. 387 (2020) 121715.
[53] M. Zhao, G.C. Fan, J.J. Chen, J.J. Shi, J.J. Zhu, Anal. Chem. 87 (2015) 12340–12347.
[54] D.M. Han, Z.Y. Ma, W.W. Zhao, J.J. Xu, H.Y. Chen, Electrochem. Commun. 35 (2013) 38–41.
[55] M. Li, R. He, S. Wang, et al., Microchim. Acta 186 (2019) 1–8.
[56] W. Wu, Z. Tan, X. Chen, et al., Biosensors 12 (2022) 130.
[57] Z.Y. Ma, J.B. Pan, C.Y. Lu, et al., Chem. Commun 50 (2014) 12088–12090.
[58] J. Luo, Y. Jiang, X. Guo, et al., Sens. Actuators B: Chem. 309 (2020) 127714.
[59] D. Cheng, H. Wu, C. Feng, Y. Ding, H. Mei, Sens. Actuators B: Chem. 353 (2022) 131108.
[60] Y. Fu, K. Xiao, Q. Zhang, et al., Anal. Chem. 94 (2022) 1874–1881.
[61] Q. Liu, J. Kim, T. Cui, in: Proceedings of the IEEE International Conference on Micro Electro Mechanical Systems, 2020, pp. 701–704, doi:10.1109/MEMS46641.2020.9056346.
[62] Q. Liu, J. Kim, T. Cui, Sens. Actuators B: Chem. 317 (2020) 128181.
[63] Y. Feng, Y. Yang, Y. Wang, et al., Sens. Actuators B: Chem. 288 (2019) 27–37.
[64] K. Wu, B. Wang, B. Tang, et al., Chin. Chem. Lett. 33 (2022) 2721–2725.
[65] R. Wang, M. Zu, S. Yang, et al., Sens. Actuators B: Chem. 270 (2018) 270–276.
[66] H. Wu, Z. Zheng, Y. Tang, et al., Sustain. Mater. Technol. 18 (2018) e00075.
[67] C. Ye, F. Xu, F. Ullah, M. Wang, Anal. Bioanal. Chem. 414 (2022) 3571–3580.
[68] L. Ge, Q. Hong, H. Li, C. Liu, F. Li, Adv. Funct. Mater. 29 (2019) 1904000.
[69] C. Wang, J. Dai, S. Guo, et al., J. Electroanal. Chem. 893 (2021) 115330.
[70] I. Ibrahim, H.N. Lim, N.M. Huang, Microchim. Acta 186 (2019) 1–11.
[71] I. Ibrahim, H.N. Lim, N.M. Huang, Z. Jiang, M. Altarawneh, J. Hazard. Mater. 391 (2020) 122248.
[72] Q. Zhang, P. Yang, J. Shen, J. Yu, J. Nanosci. Nanotechnol. 19 (2019) 7871–7878.
[73] D. Liang, X. Liang, Z. Zhang, et al., Microchem. J. 156 (2020) 104922.
[74] S. Chen, N. Hao, D. Jiang, et al., J. Electroanal. Chem. 787 (2017) 66–71.
[75] J. Du, Y. Fan, X. Gan, X. Dang, H. Zhao, Electrochim. Acta 330 (2020) 135336.
[76] Y. Ma, M. Li, Z. Li, M. Zhao, Chem. Eng. J. 431 (2022) 133880.
[77] A. Hammami, I.B. Assaker, R. Chtourou, J. Solid State Electrochem. 26 (2022) 211–218.
[78] X. Wang, X. Hu, W. Yang, et al., J. Electroanal. Chem. 895 (2021) 115536.
[79] F. Jiang, H. Tang, J. Li, L. Yang, H. Pan, Int. J. Electrochem. Sci. 15 (2020) 11976–11985.
[80] A. Levina, P.A. Lay, Chem. Res. Toxicol. 21 (2008) 563–571.
[81] W. An, X. Zhang, J. Niu, Y. Ma, Z. Han, Chin. Chem. Lett. 33 (2022) 4400–4404.
[82] J. Pang, R. Du, X. Lian, et al., Chin. Chem. Lett. 32 (2021) 2443–2447.
[83] R.S. Moakhar, G.K.L. Goh, A. Dolati, M. Ghorbani, Appl. Catal. B Environ. 201 (2017) 411–418.
[84] P. Wang, L. Cao, Y. Wu, J. Di, Microchim. Acta 185 (2018) 1–7.
[85] S. Ning, H. Lin, Y. Tong, et al., Appl. Catal. B: Environ. 204 (2017) 1–10.
[86] D. Cheng, H. Wu, C. Feng, et al., J. Alloy. Compd. 882 (2021) 160690.
[87] M. Li, G. Zhang, C. Feng, H. Wu, H. Mei, Sens. Actuators B: Chem. 305 (2020) 127449.
[88] T. Liu, B. Lin, X. Yuan, Z. Chu, W. Jin, Biosens. Bioelectron. 206 (2022) 114147.
[89] C. Song, B. Yang, Y. Zhu, Y. Yang, L. Wang, Biosens. Bioelectron. 87 (2017) 59–65.
[90] L. Zhang, L. Feng, P. Li, et al., Chem. Eng. J. 395 (2020) 125072.
[91] Z. Li, W. Dong, X. Du, G. Wen, X. Fan, Microchem. J. 152 (2020) 104259.
[92] Y. Wang, P. Wang, Y. Wu, J. Di, Sens. Actuators B: Chem. 254 (2018) 910–915.
[93] Y. Hao, Y. Cui, P. Qu, et al., Electrochim. Acta 259 (2018) 179–187.
[94] S. Wu, X. Yang, Y. Zhao, Chem. Res. Chin. Univ. 35 (2019) 370–376.
[95] L. Zhang, L. Feng, P. Li, et al., Chem. Eng. J. 409 (2021) 128154.
[96] B. Zhang, H. Wang, H. Ye, et al., Sens. Actuators B: Chem. 273 (2018) 1435–1441.
[97] S. Li, F. Zhang, L. Chen, H. Zhang, H. Li, Sens. Actuators B: Chem. 257 (2018) 9–15.
[98] B. Zhang, H. Meng, X. Wang, et al., Sens. Actuators B: Chem. 255 (2018) 2531–2537.
[99] Q. Jiang, H. Wang, X. Wei, et al., Anal. Chim. Acta 1119 (2020) 11–17.
[100] X. Zhang, M. Li, L. He, et al., J. Alloy. Compd. 864 (2021) 157905.
[101] L. Ding, Z. Dai, L. Xiao, et al., Sens. Actuators B: Chem. 339 (2021) 129871.
[102] D.M. Yang, T.F. Fu, C.S. Lin, et al., Biosens. Bioelectron. 168 (2020) 112571.
[103] H. Zhu, X. Tan, L. Tan, et al., ACS Appl. Nano Mater. 1 (2018) 2689–2698.
[104] J. Shi, J. Zhu, M. Zhao, et al., Talanta 183 (2018) 237–244.
[105] Y. Niu, G. Luo, H. Xie, et al., Microchim. Acta 186 (2019) 1–8.
[106] Q. Yu, Y. Fu, K. Xiao, et al., Anal. Chim. Acta 1195 (2022) 339456.
[107] M.H. Asif, S.M.U. Ali, O. Nur, et al., Biosens. Bioelectron. 25 (2010) 2205–2211.
[108] Y. Li, F. Chen, Z. Luan, X. Zhang, Biosens. Bioelectron. 119 (2018) 63–69.
[109] J. Hu, Z. Li, C. Zhai, L. Zeng, M. Zhu, Anal. Chim. Acta 1183 (2021) 338951.
[110] H. Deng, L. Huang, Y. Chai, R. Yuan, Y. Yuan, Anal. Chem. 91 (2019) 2861–2868.
[111] L. Huang, L. Yang, C. Zhu, et al., Sens. Actuators B: Chem. 274 (2018) 458–463.
[112] L. Chen, F. Zhang, S. Li, et al., J. Solid State Electrochem. 22 (2018) 3547–3555.
[113] C. Zhao, L. Zhang, Q. Wang, et al., ACS Appl. Mater. Interfaces 13 (2021) 20397–20404.
[114] J. Wang, Y. Zhou, L. Jiang, ACS Nano 15 (2021) 18974–19013.
[115] J. Li, X. Chang, M. Shang, et al., Ecotoxicol. Environ. Saf. 208 (2021) 111463.
[116] J. Li, Y. Li, M. Han, et al., ACS Appl. Nano Mater. 3 (2020) 9151–9157.
[117] Q. Yuan, S. Wu, C. Ye, et al., Sens. Actuators B: Chem. 285 (2019) 333–340.
[118] A. Rozov, I. Khusainov, K. El Omari, et al., Nat. Commun. 10 (2019) 1–12.
[119] A. Hazra, P. Kraft, J. Selhub, et al., Nat. Genet. 40 (2008) 1160–1162.
[120] A.K. Renfrew, E.S. O'Neill, T.W. Hambley, E.J. New, Coord. Chem. Rev. 375 (2018) 221–233.
[121] M.D.S.S. Pereira, E. Winter, J.R. Guimaraes, S. Rath, A.H. Fostier, Environ. Chem. Lett. 5 (2007) 137–141.
[122] A.J. Peter, T. Viraraghavan, Environ. Int. 31 (2005) 493–501.
[123] M. Hoang, P.J.J. Huang, J. Liu, ACS Sens. 1 (2016) 137–143.
[124] N.S. Bryan, D.D. Alexander, J.R. Coughlin, A.L. Milkowski, P. Boffetta, Food Chem. Toxicol. 50 (2012) 3646–3665.
[125] K. Rajalakshmi, S.A. John, Sens. Actuators B: Chem. 215 (2015) 119–124.
[126] K. Velusamy, S. Periyasamy, P.S. Kumar, et al., Environ. Chem. Lett. 19 (2021) 3165–3180.
[127] B. Mokhtar, T.A. Kandiel, A.Y. Ahmed, Z.R. Komy, Chemosphere 268 (2021) 128847.
[128] N. Muthuchamy, K. Lee, A. Gopalan, Biosens. Bioelectron. 89 (2017) 390–399.
[129] B. Gao, X. Zhao, Z. Liang, et al., Anal. Chem. 93 (2020) 820–827.
[130] J. Han, L. Kiss, H. Mei, et al., Chem. Rev. 121 (2021) 4678–4742.
[131] Y. Su, D. Chen, S. Yang, et al., RSC Adv. 9 (2019) 26712–26717.
[132] K. Lv, J. Chen, H. Wang, et al., Spectrochim. Acta A 177 (2017) 63–68.
[133] A. Barati, M. Shamsipur, H. Abdollahi, Sens. Actuators B: Chem. 230 (2016) 289–297.
[134] K. Shanmugaraj, M. Ilanchelian, Microchim. Acta 183 (2016) 1721–1728.
[135] D. Shchukin, D. Sviridov, A. Kulak, Sens. Actuators B: Chem. 76 (2001) 556–559.